

## Modelling the capture, by pine cones, of wind-dispersed pollen

Mohamed Lahoubi<sup>‡</sup>, Christophe Pennel<sup>‡</sup>, James E. Cresswell<sup>\*</sup>, Kevin Henning<sup>†</sup>, Michael A. Patrick<sup>§</sup>, Phillippe G. Young<sup>§</sup> and Gavin R. Tabor<sup>§</sup>

<sup>‡</sup>Institut Catholique d'Arts et Metiers, 6 rue Auber, 59046 Lille Cedex, France;

<sup>\*</sup>School of Biosciences, University of Exeter, Hatherly Laboratories, Prince of Wales Road, Exeter EX4 4PS, United Kingdom;

<sup>†</sup>University of Duisburg-Essen, Institute of Turbomachinery, Schützenbahn 70, D-45127 Essen, Germany.

<sup>§</sup>School of Engineering, Computer Science and Mathematics, Harrison Building, University of Exeter, Exeter EX4 4QF, United Kingdom

### Abstract

In this study, computational fluid dynamics (CFD) was used to simulate the dominant influences of conelet aerodynamics. To this end, airflow and particle trajectories around a virtual conelet have been visualized at a very high resolution to reveal the mechanisms of the conelet-pollen interaction. Furthermore, surfaces of the conelet have been selected to 'absorb' particles so that pollen capture could be exactly quantified. Therefore three-dimensional imaging has been introduced to obtain accurate representations of conelet morphology for aerodynamic analysis of wind pollination using CFD. The results of spore captures will be compared to results obtained for a facsimile (figure 1/) in wind tunnel experiments. Possible influence factors for pollen capture are scale camber or orientation. Series of conelets are planned to be produced, each series varying experimentally in a single feature (or more if interactions are evident). A feature is demonstrated to be a major influence if its variation is systematically associated with the aerodynamic performance of conelets.



Figure 1: Comparison between the real pine cone, the facsimile and the numerical model.

### Introduction

A fundamental objective of evolutionary biology is to explain differential diversity among lineages. Highly evident to plant biologists is the disparity in species diversity between the angiosperms (c. 300,000 species) and the 'gymnosperms' (c. 700, mainly conifers). What

accounts for the disparity? One long-established, prominent hypothesis refers to the degree of mating specificity that is conferred by the mode of pollination (biotic vs. abiotic), which we refer to as the 'pollination specificity hypothesis' (PSH). Classically, the PSH refers to the differential ability of pollination systems to reproductively isolate newly emerged genetic variants against dissolution by hybridisation, thereby influencing speciation rates /1/ /2/ /3/. Under biotic pollination, reproductive isolation arises when animal pollinators are either behaviourally faithful to floral variants (ethological isolation) or transfer the pollen of each variant using a different part of their bodies (mechanical isolation). By contrast, wind pollination, the predominant mode of abiotic pollination, is assumed to be indiscriminate and unable to contribute to reproductive isolation. This difference is used in the PSH to explain why wind-pollinated lineages have lower diversity than biotically-pollinated lineages.

Influential comparative and phylogenetic studies /4/ have shown that mode of pollination is associated with different rates of diversification among angiosperm lineages, as the PSH predicts /5/. The PSH also proposes that the preponderance of wind pollination among the gymnosperms explains their low diversity relative to the angiosperms, but this is hotly contested /6/. Moreover, the premises of the PSH have yet to be fully validated in this context. Whereas reproductive isolation through plant-pollinator interaction has been demonstrated experimentally /7/, it is simply asserted as self-evident that wind-pollination is indiscriminate. If, however, wind pollination can promote reproductive isolation, particularly in gymnosperms, this would call the PSH into question.

### The study of Karl Niklas.

Karl Niklas studied the aerodynamical behavior of pine cones for different species in the 1980's /8/ /9/. Actually, he gave some explanation relative to the morphological phenomenon in the reproduction mechanisms. As an example, he noticed that there is

more probability for a conelet to capture a pollen grain from its own specie than from another one. In fact, the morphological pollen grains “correspond” to the ovulate receptors. Karl Niklas studied different characteristics of the pine cone’s environment (pine cone’s inclination, wind velocities and orientation, needles influence, height in the tree etc.).

He made a papier-maché model representing a pine cone of a *Pinus* in order to simulate the wind-pollination, to see how many particles are trapped and which way they follow before their capture. For this reason, he put the paper model into a wind tunnel, injected helium bubbles into the flow to simulate the pollen grains and visualized them. In fact, he noticed that there are more trapped particles on the back of the cone than on the front.

In 1984, Niklas did experiments with a Reynolds number of 264. He studied the three dimensional airflow patterns and noticed the following data concerning the Reynolds number:

- The leeward airflows are unstable and some eddies alternatively detach from the model. The wakes following the separated region are in the  $x$ - $y$  plane. Each successive vortex rotates in a direction opposite its predecessor.
- The airflow passing laterally around the cone produces a wake of vortices in the  $x$ - $z$  plane. The vortices from the upper side rotate clockwise and the lower vortices rotate counter clockwise.

Niklas noticed that the airflow (around an ovulate cone) conforms to a symmetrical leeward umbilicus pattern. This pattern is folding inward at the midpoint of the pine cone’s longitudinal axis /figure 2/. He also noticed, that this umbilicus pattern is oscillating with a predictable frequency. It appears as bursts of eddies alternating from the bottom to the top of the pine cone. In normal orientation the umbilicus covers approximately the middle-third of the downwind surface of the pine cone.

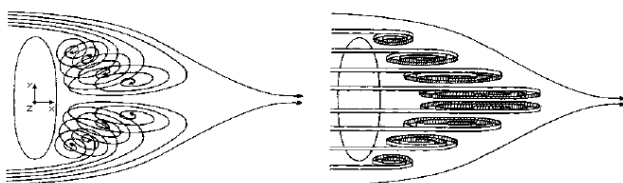


Figure 2: Draft made by Karl Niklas showing the leeward umbilicus pattern.

The vortices, in distal and proximal portion, are smaller and move more rapidly than the ones produced along the lateral surfaces. The airflow which is passing over the pine cone is progressively more elliptical and moving at a slower speed when it is directed toward the cone. Usually, airflow speed gradually decelerates along the streamlines as they are deflected backward. Karl Niklas was also able to find out, that the ovulate cone deflects pollen grains passing over its surfaces into trajectories that are directed back toward the cone surface. Dependent upon the geometry of the cone and the ambient airflow speed, there exists a boundary layer effect that defines which of two general types of

trajectories a pollen grain takes. Pollen grains passing by the cone within this geometry are deflected backward and will have a high probability of settling on or impacting with cone scales. Pollen grains passing by the cone at a distance equal to or greater than the umbilicus surface will be deflected back toward the cone, but will decelerate and fall downward, becoming re-entrained by airflow passing under the cone.

Concerning this result, he claimed that his model was a viable compromise in aerodynamic scaling. It permitted a first approximation of the pollen behaviour through the helium bubbles motions. He noticed that the pollen particles would follow a backwind eddy which first passed the cone and then flowed between downwind scale-bract complexes. Usually, he saw a general cyclonic air disturbance pattern going toward the inside scale bracts. Moreover, Niklas noticed that the phenomenon most frequently observed are doldrums like eddies over the adaxial surface of the scales. He saw that the airflow is directed between two superimposed scales bract complexes. So the helium bubbles enter along the abaxial surface and move toward the position of the ovules. Karl Niklas concluded that two processes account for pollen capture by the cones:

1. *The turbine hypothesis.*

The helical arrangement of the cone scales acts as a turbine to channel air into a cyclonic vortex among the scales so that airborne pollen failing to adhere to one scale passes to the next, thus increasing the effectiveness of its capture /figure 3/.



Figure 3: The turbine effect.

2. *The recirculation hypothesis.*

The conelet creates back-sweeping eddies that recirculate air over the leeward surfaces. Pollen entering this eddy is deflected between the leeward scales, thus enabling its capture /figure 4/.



Figure 4: The leeward effect.

Although these results describe in detail the flow field at a conelet, they do not explain how selectivity is achieved. The aerodynamic behaviour of particles is determined largely by their size, shape, and density, which are characterised by their 'settling velocity' (terminal velocity in still air). Even if conelets are aerodynamically tuned to capture a particular kind of particle, they should nevertheless capture similar particles more than dissimilar ones. However, analysis of Niklas' data finds no relationship among species between their propensity to capture each other's pollen and the relative similarity of their pollen. Therefore, although it is most likely that conelets are tuned to pollen size, shape and density, this is currently unproven.

### Solution Method

The governing Navier-Stokes-Equations were solved with the segregated, implicit solver for incompressible flow and an absolute velocity formulation was chosen. The calculation was made in single precision mode with a 2<sup>nd</sup> order accurate discretisation in space and time. For the pressure-velocity coupling the SIMPLE-method was used. For the three-dimensional computational domain air was assumed to be the working fluid. In addition gravitation in the y-direction was added with a value of  $-9.81 \text{ m/s}^2$ . The Reynolds' number which Karl Niklas used was 264 [9]. The *cedrus libani* had a length of 8 mm, the density of air at 300 K was  $1.225 \text{ kg/m}^3$  and the dynamic viscosity  $1.7894 \cdot 10^{-5} \text{ Pa} \cdot \text{s}$ , so the velocity at the inlet, for a Reynolds number of 264, had to be  $0.482 \text{ m/s}$ .

The type of the outer boundary conditions of the calculation area are shown in /table 1/. The pressure outlet was used with its default settings. The pine cone's surface was set to "wall". All faces which are not mentioned in this script were set to "interior".

The time step size at the beginning of the calculation was  $10^{-7} \text{ s}$  and could be enlarged each time after 10 steps by one increment up to a maximum of  $10^{-3} \text{ s}$  per time step.

Table 1: Boundary Conditions

Velocity Inlet	0,482 m/s
Pressure Outlet	0 Pa
Time Step Size	$10^{-3} \text{ s}$
Time Steps	1000

To receive information about the behaviour of the pine cone model pertaining to pollen capture, injections of inert particles into the calculation area were made after a simulated time of 1 s. For this, 10 injection groups were defined from where the pollen was released. Four different cases were simulated, each one with spherical particles of  $60 \mu\text{m}$  in diameter, but different densities.

1. Helium bubbles:  $\rho_1 = 0.1625 \text{ kg/m}^3$
2. Pollen grains:  $\rho_2 = 250 \text{ kg/m}^3$
3. Pollen grains:  $\rho_3 = 500 \text{ kg/m}^3$
4. Pollen grains:  $\rho_4 = 750 \text{ kg/m}^3$

To know which particles were captured, the wall boundaries of the pine cone had to be given a special setting. In this study two types of different wall-boundaries were used: "Wall-Trap" boundaries /figure 6/ and "wall-reflect" boundaries /figure 7/. Due to the fact that the pollen are settling down on the adaxial surface of the scales, only the adaxial faces of the backsides of the scales were set to trap particles. All the other faces of the pine cone were set to reflect them. For this, 24 equally distributed trap boundaries were made for statistical reason and one reflect boundary for the rest of the pine cone. With this set of boundary conditions, it was possible to receive the distribution of the trapped particles to find out at which sides the model is capturing more or less of them. For each case 1000 particles (100 of each group) were released.

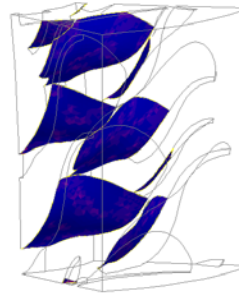


Figure 6: Wall-Trap Boundary condition faces.



Figure 7: Wall-Reflect Boundary condition faces.

### Results

The vectors coloured by velocity magnitude and shown in /figure 8/ display a good agreement with the drawing of Karl Niklas /figure 2/. In both pictures the eddies within the umbilicus are visible, but unlike the Niklas pine cone, no alternation can be found for the numerical model. The upper vortices rotate clockwise while the lower ones rotate counter clockwise. The two large vortices of the wake found in /figure 8/ and /figure 9/ could influence the trajectories of the pollen grains and transport them back to the leeward surface of the pine cone, so they could render possible the pollen capture on the backside of the numerical model.

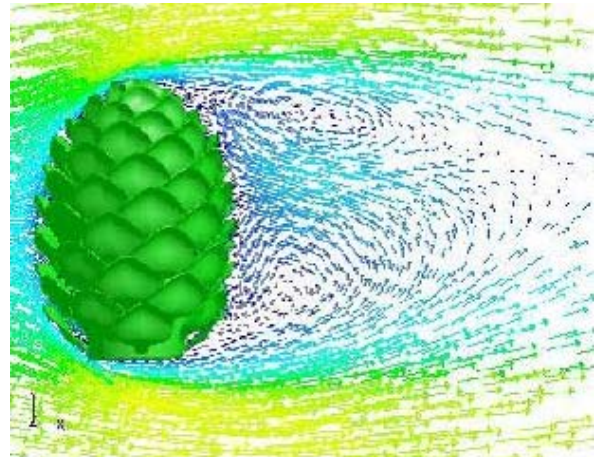


Figure 8: Vectors coloured by velocity magnitude in the xy-plane.

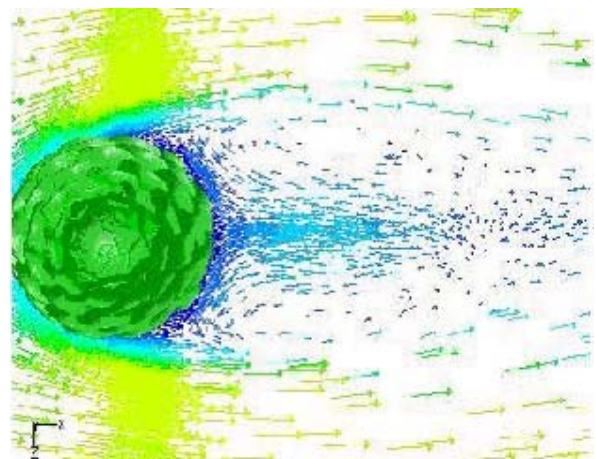


Figure 9: Vectors coloured by velocity magnitude in the xz-plane.

The trajectories of the injected helium bubbles ( $\rho_1$ ) completely surround the pine cone. Only a few touched it but did not proceed into it. A leeward effect can be seen at the backside of the cone, but no particles were trapped. They circled one time in the wake before they proceeded downstream to leave the calculation area.

The second case /figure 10/ and /figure 11/ for particles with 250 kg/m<sup>3</sup> ( $\rho_2$ ), shows that the injected pollen grain inertia was too high to follow the air around the pine cone, which resulted in a collision. The lower sides of the scales seem to perfectly deflect the grains into areas of low velocities. Especially at the stagnation point, they were very effective in doing so. Inside the cone the grains could settle down on the backsides of the scales. At the backside of the cone, about 0.4 % of the particles were circling in the wake but did not hit the pine cone, so a leeward effect could not be found.

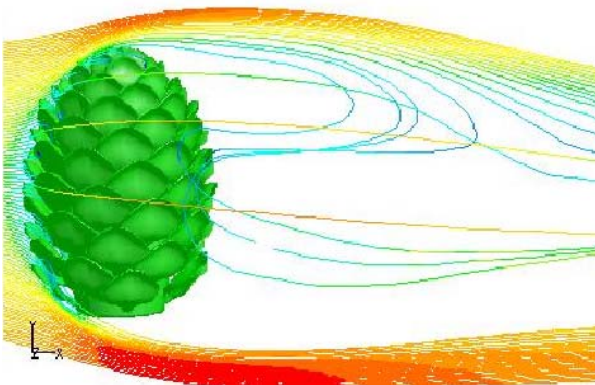


Figure 10: Particle trajectories in the xy-plane.

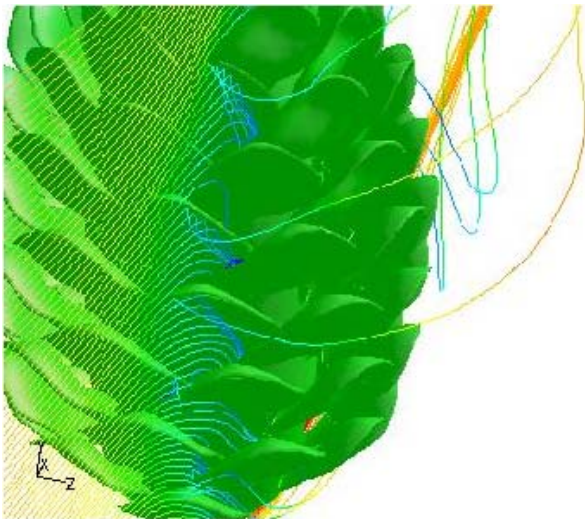


Figure 9: Particle trajectories in detailed isometric view.

The third case ( $\rho_3$ ) shows that with higher density more pollen grains hit the pine cone instead of orbiting it. They were reducing their velocity by bouncing a couple of times between the scales. About 5 % of the particles bounced out of the pine cone again, but most of them were captured. At the backside of the cone, only 0.5 % of the grains were circling in the wake but only one seemed to hit the pine cone, so a leeward effect could not be found.

The fourth case ( $\rho_4$ ) shows that with still higher density even more pollen grains hit the pine cone instead of orbiting it. They were again reducing their velocity by bouncing a couple of times between the scales. It seems that about 8% of the grains bounced out of the pine cone again. At the backside of the cone, 0.7% of the grains were circling in the wake but none of them seemed to hit the pine cone, so a leeward effect could not be found.

### Particle trapping rates

#### 1. Helium Bubbles: $\rho_1 = 0.1625 \text{ kg/m}^3$ :

Total Capture = 0.0 %

The model did not catch any of the helium particles.

#### 2. Pollen Grains: $\rho_2 = 250 \text{ kg/m}^3$ :

Total Capture = 8.3 %

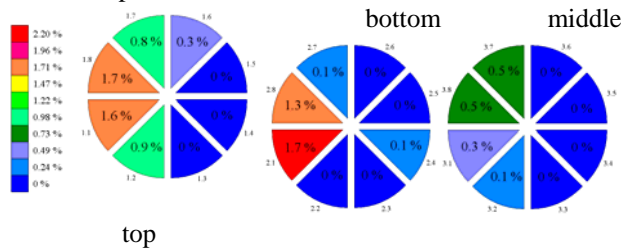


Figure 10: Pollen grain capture of the 3 x 8 pieces of the pine cone with airflow from left to right.

In /figure 10/ can be seen that the model caught the particles especially at the centre of the model's front side. Only one particle was captured at the backside, so it can be assumed that there was no leeward effect for this particle density. There was only one outlier (piece 1.2) but, probably as a result of the scales orientation relative to the flow, a few particles were able to leave piece 1.1 and were caught by the next piece which is 1.2.

#### 3. Pollen Grains: $\rho_3 = 500 \text{ kg/m}^3$ :

Total Capture = 13.9 %

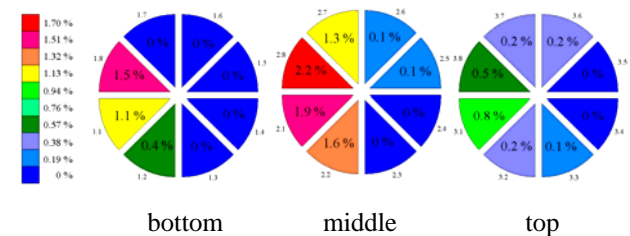


Figure 11: Pollen grain capture of the 3 x 8 pieces of the pine cone with airflow from left to right.

In /figure 11/ can be seen that the model caught most particles at the model's front side. The capture was more balanced between the four front side pieces but there was still an overbalance at the centred pieces (n.1 and n.8; n = 1, 2, 3). Only few particles were

captured at the backside of the model, so it can be assumed that there was no leeward effect for this particle density. There were two outliers at the top (piece 3.7 and 3.8), probably as a result of the scale orientation relative to the airflow.

#### 4. Pollen Grains: $\rho_4 = 750 \text{ kg/m}^3$ :

Total Capture = 14.7 %

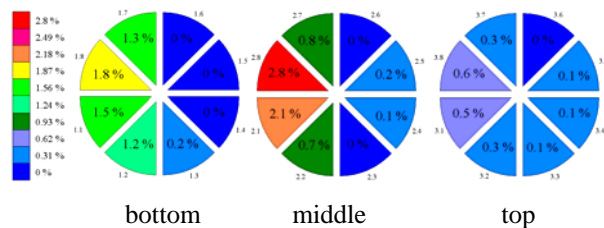


Figure 12: Pollen grain capture of the 3 x 8 pieces of the pine cone with airflow from left to right.

In /figure 12/ can be seen that the model caught nearly all particles at the model's front side. The capture was balanced between the four front side pieces but there was still an overbalance at the centred pieces (n.1 and n.8; n = 1, 2, 3) especially in the middle part. Rarely particles were captured at the backside of the model, so it can be assumed that there was no leeward effect for this particle density.

To summarise, it can be said that this pine cone model captures the heavier particles better than the light ones. The highest degree of efficiency is about 15 % for a particle density of about  $750 \text{ kg/m}^3$  as shown in /figure 13/. Unfortunately, the density of the *Cedrus libani* pollen is not known, but considering the present results it can be expected to be about  $750 \text{ kg/m}^3$  or higher.

The model has the best trapping rate at its stagnation point and with increasing density, the pine cone uses more and more of its front side projection screen for trapping particles as shown in /figure 11/ and /figure 12/. At the backside of the model the trapping rate never exceeds a value of 0.8 %.

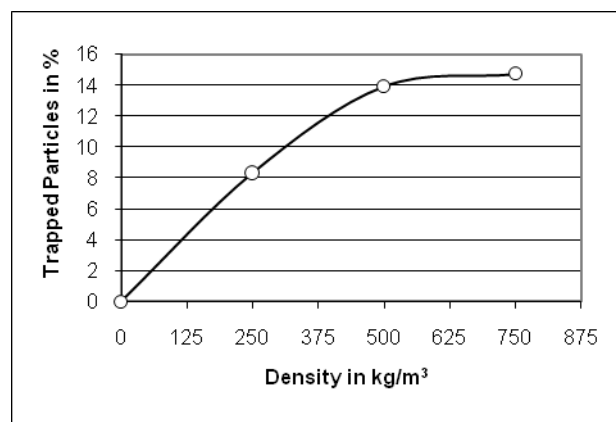


Figure 13: Trapping rates of the pine cone model for different particle densities

#### Conclusion

In view of the fact that the results of this study didn't show any of the effects described by Karl Niklas, the conclusion must be that different types of pine cone probably use different methods for trapping particles. Especially the fact that this model did not capture any of the helium bubbles injected into the calculation area, shows that this pine cone does not capture pollen in the same way as in the Niklas model. Whereas his model caught most of the particles at its backside, the numerical model caught most of them at its front side. Instead of trapping pollen by some kind of leeward effect, the *Cedrus libani* probably uses its scales to create a pocket-like gap in which the particles are deflected. The grains are not retiring in a doldrum-like eddy, they simply fall on the backside of the scales. Furthermore, the trapping rate of the numerical model increases with increasing particle density /figure 13/, which can be seen as a first step of separation. So pollen density is probably one aspect of differentiation between pollen from its own and the pollen of other species.

A next step for this kind of study can be to improve the scale shape. Maybe the degree of efficiency can be increased with scales still closer to reality or maybe the differentiation between the pollens can be improved, because even small changes in the scale shape can have big influences on the shape of the whole pine cone.

Another possibility could be to create a numerical facsimile of the Niklas model. If it is possible to simulate the leeward effect, maybe it is possible to explain the mechanisms which cause it. At the same time, a simulated Niklas model would give a better reference to further studies and it would sustain the thesis of different types of trapping methods. Maybe there are more than just two of them and maybe the turbine effect plays an important role in this phenomenon. The different effects might be used for different areas of pollen density.

#### References

- /1/ Grant, V. : Pollination systems as isolating mechanisms in angiosperms. *Evolution*, 3, (1949), 82-97.
- /2/ Stebbins, G.L.: Why are there so many species of flowering plants? *Bioscience*, 31, (1981), 573-577.
- /3/ Crepet, W.L. : Advanced (constant) insect pollination mechanisms: patterns of evolution and implications *vis-a-vis* angiosperm diversity. *Annals Of The Missouri Botanical Garden*, 71, (1984), 607-630.
- /4/ Dodd, M.E., Silvertown, J. & Chase, M.W.: Phylogenetic analysis of trait evolution and species diversity variation among angiosperm families. *Evolution*, 53, (1999), 732-744.
- /5/ Bolmgren, K., Eriksson, O. & Linder, H.P.: Contrasting flowering phenology and species richness in abiotically and biotically pollinated angiosperms. *Evolution*, 57, (2003), 2001-2011.

- /6/ Gorelick, R.: Did insect pollination cause increased seed plant diversity? *Biological Journal of the Linnean Society.*, 74, (2001), 407-427.
- /7/ Fulton, M. & Hodges, S.A.: Floral isolation between *Aquilegia formosa* and *Aquilegia pubescens*. *Proceedings of the Royal Society of London. B*, 266, (1999), 2247-2252.
- /8/ Niklas, K. J.: Conifer Ovulate Cone Morphology: Implications on Pollen Impaction. *American Journal of Botany*, Vol. 70, No. 4 (Apr., 1983), 568-577.
- /9/ Niklas, K. J.: The Motion of Windborne Pollen Grains Around Conifer Ovulate Cones: Implications on Wind Pollination. *American Journal of Botany*, Vol. 71, No. 3 (Mar., 1984), 356-374.